Applied Environmental Research

Journal homepage : http://www.tci-thaijo.org/index.php/aer

Biochar from Rice Husk as Efficient Biosorbent for Procion Red Removal from Aqueous Systems

Neza Rahayu Palapa[1], Tarmizi Taher[2,3], Novie Juleanti[4], Normah[4] Aldes Lesbani[1,3,*]

[1] Graduate School of Mathematics and Natural Sciences, Sriwijaya University, South Sumatra, Indonesia
[2] Department of Environmental Engineering, Institut Teknologi Sumatera, Lampung Selatan, Indonesia
[3] Research Center of Inorganic Materials and Coordination Complexes,
Faculty of Mathematics and Natural Sciences, Universitas Sriwijaya, Ogan Ilir, Indonesia
[4] Magister programme, Faculty of Mathematic and Natural Sciences,
Sriwijaya University, Ogan Ilir, South Sumatra, Indonesia
[*] Corresponding author: aldeslesbani@pps.unsri.ac.id

Article History
Submitted: 12 October 2020/ Revision received: 10 February 2021/ Accepted: 12 February 2021/ Published online: 27 July 2021

Abstract

Numerous reports have elucidated the use of biochar (BC) to adsorb dyes from wastewater. However, its applicability for adsorbing Procion Red, which causes carcinogenic and mutagenic effects on aquatic life, has not been studied. In this work, biochar produced from rice husk in Sumatera, Indonesia was used as a biosorbent for Procion Red removal from aqueous systems. Rice husk-BC was characterised using X-ray diffraction (XRD), Fourier transform infrared (FTIR) spectroscopy, surface area specific analysis, and scanning electron microscopy (SEM) for morphological analysis. The characterisation showed a (002) reflection peak at 2θ = 23° with broad and quite intense diffraction, which indicates reflection of electromagnetic waves by silicates, oxides and carbon present in the rice husk-BC. The surface area and SEM morphologies confirm that after pyrolysis, the surface of the rice husk changed. The FTIR spectra confirm the presence of functional groups such as the carboxylic acids and aromatic compounds. The surface area of rice husk-BC was up to ten times that of its raw material. The results of adsorption studies indicate that adsorption of Procion Red on rice husk-BC follows a pseudo-second-order (PSO) reaction with a rate constant of 0.044 min^{-1} and Langmuir isotherm models with a coefficient of correlation close to unity. The maximum adsorption capacity increased from 36.900 mg g^{-1} for the rice husk to 84.034 for the rice husk-BC. Thermodynamic analysis showed positive enthalpy and entropy, indicating that Procion Red adsorption is endothermic; thus, the Gibbs energy values decreased with increase in temperature, indicating that high temperatures are favourable for the adsorption process. Furthermore, the study of adsorption of Procion Red on rice husk-BC and regeneration of the adsorption capacity of rice husk-BC showed the largest drop in the fourth and last cycle.

Keywords: Adsorption; Procion red; BC; Bio-sorbent; Biosorption; Rice husk

https://doi.org/10.35762/AER.2021.43.3.6

Introduction

It is important to solve the environmental problems caused by synthetic dyes [1]. Sources of contaminant dyes include textile industries [2], paper industries, pulp industries, and cosmetic industries [3–4]. Synthetic dyes are harmful to the environment, not easily biodegradable, highly toxic, and are highly dispersible in surface water [5–6]. The removal of dye molecules from wastewater is important, and it is very interesting to see how this can be achieved [7]. Treatment methods to remove dyes from wastewater, including photodegradation [8], bioremediation [9], decomposition [10], and adsorption, have been examined [11–13]. Among these, adsorption is more popular because of its low setting-up cost, ease of operation, and high efficiency [14].

The presence of synthetic dyes such as Procion Red in wastewater causes carcinogenic and mutagenic effects on aquatic life as well as environmental damage [15]; this prompted Scientists to conduct research on the removal of Procion Red from wastewater through adsorption methods. As reported in Nazifa et al [16], the use of activated carbon from corncob to remove Procion Red resulted in a maximum adsorption capacity of 2.86 mg g^{-1}. Another research by Sarma et al. [17] using montmorillonite to remove Procion Red produced a maximum adsorption capacity of 11.09 mg g^{-1}, while Procion Red adsorption using commercial activated carbon resulted in a maximum adsorption capacity of 167 mg g^{-1} at 273 K [18]. Biosorbent from modified avocado shells was also found to be highly effective for Procion Red removal, with a maximum adsorption capacity of 167 mg g^{-1} [19].

A material has greater potential for use as an effective adsorbent if it has high adsorbance properties, larger number of active sites on the surface, and high stability during preparation [20]. Biosorbents from natural biomass yield inexpensive adsorbents [21]. However, the disadvantages of natural materials are that they have active sites on the surface, and low adsorption capacity [22]. Therefore, there is a growing need to find new adsorbents for practical applications that are economical, easily available, and effective. Natural, carbon-rich materials known as biochar (BC) or hydrochar have been found to be effective and renewable [20, 23]. In recent years, researchers have explored BC or hydrochar from natural materials such as wheat [24], coconut shell [25], wheat straw [26], peat husk [27], sawdust [28] and rice husk, as adsorbents. Rice husk is a low-cost and environment-friendly biomass, nearly 26 million tons of which is produced every year in Indonesia [29]. Rice husk has a hard surface and high silicon content, making it difficult to decompose; the main components of rice husk are cellulose, lignin, and silicon [30]. BC from rice husk is a porous material with a large specific surface area and contains rich functional groups on the active sites [31–32]. Thus, BC from rice husk can be used as an adsorbent with economic potential for the removal of heavy metal cations and organic contaminants from wastewater. Several studies have used BC to adsorb dyes from wastewater. According to Leng et al. [31], when BC from rice husk was utilized to remove malachite green dye from aqueous solutions it indicated an adsorption capacity of 67.7 mg g^{-1}. Chen et al. [32] reported that direct red dye had been removed by rice husk-BC at an adsorption capacity of 59.77 mg g^{-1}. Rice husk-BC was also used to adsorb methylene blue from aqueous solutions, and it reached an adsorption capacity of 17.92 mg g^{-1} [33]. Luyen et al. [34] reported the use of rice husk-BC nanocomposite in another case to remove crystal violet from wastewater, where the adsorption capacity reached 185 mg g^{-1}. For comparison, adsorption of Procion Red was studied using inorganic materials such as bentonite clay [35]. The adsorption capacity was 5.26 mg g^{-1} for natural bentonite and 9.97 mg g^{-1} for activated bentonite. Similar results were obtained by Sarma [17] when montmorillonite was used as the adsorbent to remove Procion Red from an aqueous solution; the adsorption capacity was found to be 11.04 mg g^{-1}. Based on these results, it can be concluded that biochar is a more effective adsorbent with higher adsorptivity for Procion Red and higher reusability compared to those of other materials, especially clay. In this study, the experiments on adsorption were conducted with adsorbents and Procion Red to determine adsorption times, Procion Red concentration, and adsorption temperature setting. The regeneration capacity of the adsorbent was also studied from an economic point of view, for industrial and large-scale practical applications.

Materials and Methods

1) Chemicals

Procion Red, the chemical formula of which is $C_{19}H_{10}Cl_2N_6Na_2O_7S_2$, was purchased from Sigma Aldrich. All chemicals used were of analytical grade from Merck, including absolute ethanol, sodium hydroxide, and hydrochloric acid. Rice husk was procured from paddy fields in Indonesia through Bukata Organics, Indonesia.

2) Biochar preparation

Rice husk-BC was produced through thermal treatment of the rice husk; the thermal treatment was carried out in a furnace at 600 °C under nitrogen flow (10 °C min^{-1}) for 2 h. Thereafter, the reactor was cooled down and the prepared BC was characterised. This was done through X-ray diffraction (XRD) using a Rigaku Miniflex-600 diffractometer, Fourier transform infrared (FTIR) spectroscopy using a Shimadzu Prestige-21 spectrophotometer, morphology analysis using a Quanta-650 Oxford instrument scanning electron microscope (SEM), and BET using a micrometrics instrument by ASAP Micromeritics 2020. The BC thus prepared was used in the adsorption experiments.

3) Adsorption experiments

Adsorption experiments to determine the effect of adsorption time, initial concentration of Procion Red, and temperature on the efficiency of adsorption Procion Red as well as to determine the adsorption isotherm, adsorption kinetics, and adsorption thermodynamics, were conducted. This procedure was carried out for various initial concentrations up to 50 mg of rice husk-BC and rice husk was added to 50 mL each of Procion Red solution, and the batch shaken for 5–180 min at 303–333 K; this procedure was carried out for various initial concentrations of the dye. Concentration of the adsorption process was tested using a UV–vis spectrophotometer at 537 nm. The desorption process was induced using a hydrochloric acid solution (0.01 M), sodium hydroxide solution (0.01 M), water, and ethanol (absolute for analysis). Reusability was tested by adding 1 g of the adsorbents (i.e. rice husk and rice husk-BC) separately to 50 mL of Procion Red solution, the concentration of which was 100 mg L^{-1}; then, the mixture was shook for 2 h. The dried adsorbent was reused for four cycles through procedures similar to those in the first adsorption experiments.

Results and discussion

1) Adsorbent characterisation

Rice husk-BC was characterised by XRD, FTIR, SEM, and BET surface area measurements. The results of the XRD analysis of the rice husk and rice husk-BC are depicted in Figure 1. The XRD pattern shows that rice husk and rice husk-BC have an amorphous regions corresponding to their lignin content. According to Ntaflou and Vakros [36], the broad peak at 23° corresponding to 2θ indicated the presence of carbon-rich materials with less ordered structures due to pyrolysis. Peaks of other raw materials indicate lignin and cellulose [37]; however, after pyrolysis, the peaks related to lignin and cellulose disappeared [38].

The FTIR spectra showed indicated presence of hydroxide groups, with transmittance/ absorbance of wave numbers ranging from 3400 and 3448 cm^{-1} The FTIR spectra showed hydroxide groups stretching to 3448 cm^{-1}. The low transmittance/absorbance at 794 cm^{-1} indicated C-H ring deformation or C-H wagging [39]. Other vibration bands at 1103 cm^{-1} are attributed to silicate oxide; 1620 cm^{-1} denotes the formation of functional groups with oxygen, such as carboxyl C=O stretching and aromatic C=C stretching.

The morphologies of the rice husk and rice husk-BC are captured in Figure 2. The morphology of the rice husk indicates homo-globular particles when zooming to 30.0 µm, assumed to be the lemma and palea components of the rice husk [40]; the rice husk-BC morphology showed some pores due to pyrolysis at temperatures above 500 °C. However, other researchers who conducted the experiment at temperatures lower than 500 °C noted that during pyrolysis the hetero pores and the pores were not fully developed [41].

The specific surface areas and porosities of rice husk and rice husk-BC are listed in Table 1. Table 1 shows that the specific surface area of rice husk increased significantly after pyrolysis. This indicates that upon heating, the volatilisation of organic compounds in the rice husk created BC with a porous structure, resulting in a much higher surface area. The average pore size of the rice husk-BC also increased due to the higher temperature during heating. As reported by Shi et al [38], there was a dramatic increase in the number of larger pores in the rice husk-BC samples, due to the high temperature prevailing during pyrolysis.

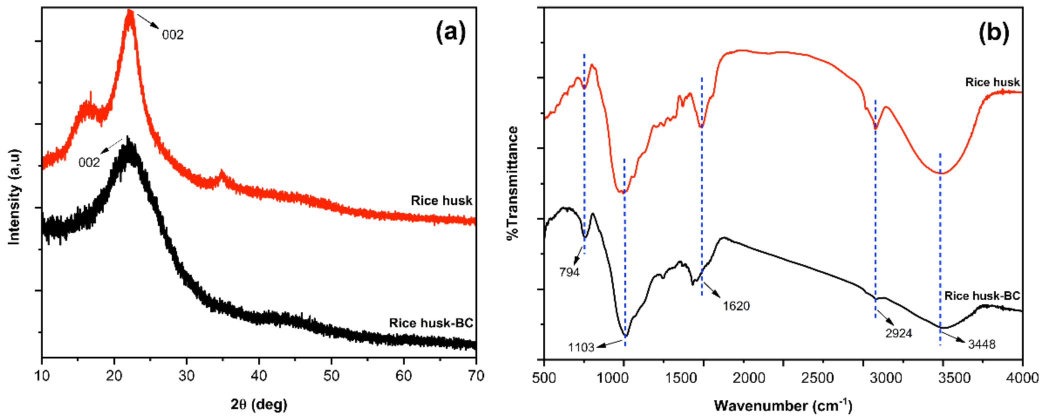

Figure 1 Pictures of XRD powder pattern (a) and FT-IR spectrum (b) of rice husk and rice husk-BC.

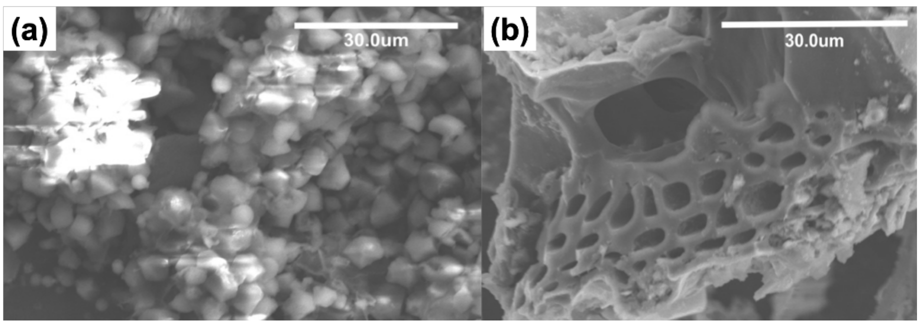

Figure 2 Morphological images of rice husk (a) and rice husk-BC(b).

Table 1 Specific surface area and porosity of rice husk and rice husk-BC

Adsorbent	Surface Area ($m^2 g^{-1}$)	Pore Size (nm)	Pore Volume ($cm^3 g^{-1}$)
Rice husk-BC	72.25	3.33	0.060
Rice husk	7.08	3.14	0.011

2) Adsorption behaviour of adsorbents

The contact time of the adsorption process is an important parameter to be determined; the dye uptake increased slightly with time till it reached an equilibrium. The adsorption of Procion Red using both rice husk and rice husk-BC indicated equilibrium conditions after 120 min contact time; at this stage, rice husk-BC had an adsorption capacity of 25.190 mg g^{-1}, and rice husk had 18.354 mg g^{-1}. The increase in adsorption capacity up to the equilibrium state was caused by the adsorption ability of active sites on the adsorbent surface, which was rich in pores, as well as large magnitude of unbalanced molecular forces during the initial contact time as well [42]. The results of the adsorption time experiment are shown in Figure 3, while Table 2 presents the kinetics of Procion Red adsorption using rice husk-BC and rice husk. The kinetic model is described by the pseudo-first-order (PFO) pseudo-second-order (PSO) and Elovich models.

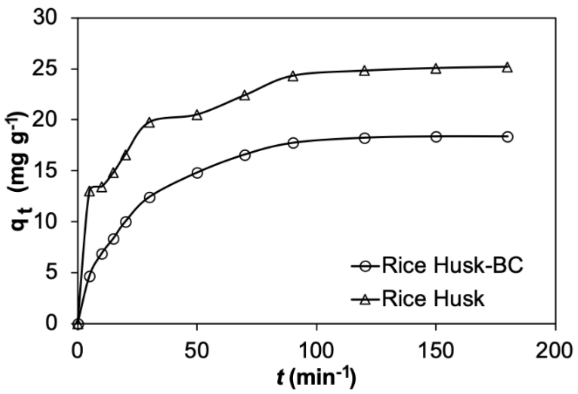

Figure 3 Effect of time adsorption of procion red removal onto rice husk-BC and rice husk.

The kinetics of the adsorption process was determined using three most studied kinetic models, which can be expressed as:

$$\log (q_e\text{-}q_t) = \log q_e - \left(\frac{k_1}{2,303}\right) t \qquad \text{(Eq. 1)}$$

$$\frac{t}{qt} = \frac{1}{k2qe^2} + \frac{1}{qe} t \qquad \text{(Eq. 2)}$$

$$q_t = \frac{1}{b} \ln ab + \frac{1}{b} \ln t \qquad \text{(Eq. 3)}$$

where q_e is the adsorption capacity at equilibrium (mg g^{-1}), q_t is the adsorption capacity at time t (mg g^{-1}), t is the adsorption time (min^{-1}), k_1 is the adsorption kinetic rate at pseudo-first-order (min^{-1}), and k_2 is the adsorption kinetic rate at pseudo second-order (g mg^{-1} min^{-1}); a is Elovich adsorption rate, b is Elovich constants (g mg^{-1} min^{-1}).

According to Table 2, the kinetics model is explained better by PSO compared to PFO and Elovich; values calculated using PSO are a better match with observed with observed values (with $R^2 > 0.996$). For both rice husk and rice husk-BC kinetic data, the k_1 value was obtained by plotting ln(qe−qt) against t; the k_2 value by plotting t qt^{-1} against t; and the a and b by plotting q_t vs. ln t as written by Eq. 1–3. The adsorption capacity of rice husk-BC was greater than that of rice husk because of the higher surface area and pore size of the BC. The adsorption of rice husk-BC and rice husk reached equilibrium after 70 and 90 min, respectively; it is assumed that the process to remove Procion Red is quicker on rice husk-BC than on rice husk [43]. However, the porous structure of rice husk-BC may have resulted in longer intraparticle diffusion path and slower kinetics, compared with those in rice husk. In Figure 3, the symbols denote experimental values of q_t, and solid lines denote q_t calculated using kinetic parameters including PFO and PSO; Elovich described the activation chemisorption energy of adsorption; q_t corresponding to the PSO parameter is close to the experimental value of q_t for rice husk and rice husk-BC, respectively. All the kinetics parameter data are listed in Table 2. The experiments successfully demonstrated that the removal of Procion Red reached 99% sing rice husk-BC and 62% percent using rice husk, 3 h from the time initial concentration of Procion Red was 25 mg L^{-1}.

Table 2 Kinetic adsorption results for Procion Red

Parameters		Adsorbent	
		Rice husk	**Rice husk-BC**
PFO	q_e	17.254	17.697
	k_1 (min^{-1})	0.025	0.033
	R^2	0.990	0.992
PSO	q_e (mg g^{-1})	20.747	26.954
	k_2 (mg min^{-1})	0.022	0.044
	R^2	0.996	0.999
Elovich	a (g mg^{-1})	0.472	0.363
	b (g mg^{-1} min^{-1})	0.25	0.234
	R^2	0.9657	0.979

The graphs describe the effect of the initial concentration and temperature on the equilibrium state of the adsorption process. Table 3 and Figure 4 show the results of the Langmuir and Freundlich models that were tested in this experiment; these isotherm models are formulated as expressed in Eq. 3 and 4:

$$\frac{1}{q_e} = \frac{1}{q_{max}} + \frac{1}{q_{max}b} \cdot \frac{1}{C_e} \quad \text{(Eq. 4)}$$

$$\ln q_e = \ln K_f + \left(\frac{1}{n}\right) \ln C_e \quad \text{(Eq. 5)}$$

where q_{max} is the maximum adsorption capacity of the monolayer (mg g^{-1}), b is the Langmuir adsorption equilibrium constant (mg^{-1}), C_e is the equilibrium concentration (mg L^{-1}), and K_f is the Freundlich constant. The equilibrium of the process was analysed using the Langmuir isotherm, where q_{max} was obtained from the intercept and slope of the plot of q_e C_e^{-1} vs. q_e using the Langmuir adsorption isotherm (as shown in Eq. 4). The values of K_F and n were obtained from the intercept and slope of the line obtained by plotting ln q_e versus ln C_e as Eq. 5. Figure 3 shows that the adsorption capacities increase with increasing temperature. This finding indicates that conditions are favourable for adsorption at high temperatures, and adsorbents occupy inactive sites as the saturation value is reached [44]. Thus, the efficiency of removal of Procion Red increases with increasing temperature, with the adsorption capacity increasing up to a temperature of 333 K. Increasing amount of adsorbed Procion Red with increasing temperature suggests the endothermic nature of the adsorption process and the primary role of temperature in the removal of Procion Red [45]. An increase in temperature is known not only to increase the diffusion rate of the intermediate molecules across the external boundary layer and within the pores, but also to modify the equilibrium capacity of the adsorbent for a particular adsorbate. Based on the coefficient of determination, the best-fit isotherm model in this experiment is Langmuir, which indicates the monolayer adsorption process.

Table 3 shows the increase in Q_{max} of rice husk-BC from 36.900 mg g^{-1} to 84.034 mg g^{-1}. These Q_{max} values are comparable to those of other biosorbents used as Procion Red removal agents such as *Bacillus subtilis* [15], activated pine fruit shell [46], Res. *Deffated Nigrospora* Sp [47], spirulina algae [11] and layered double hydroxide [48], as listed in Table 4.

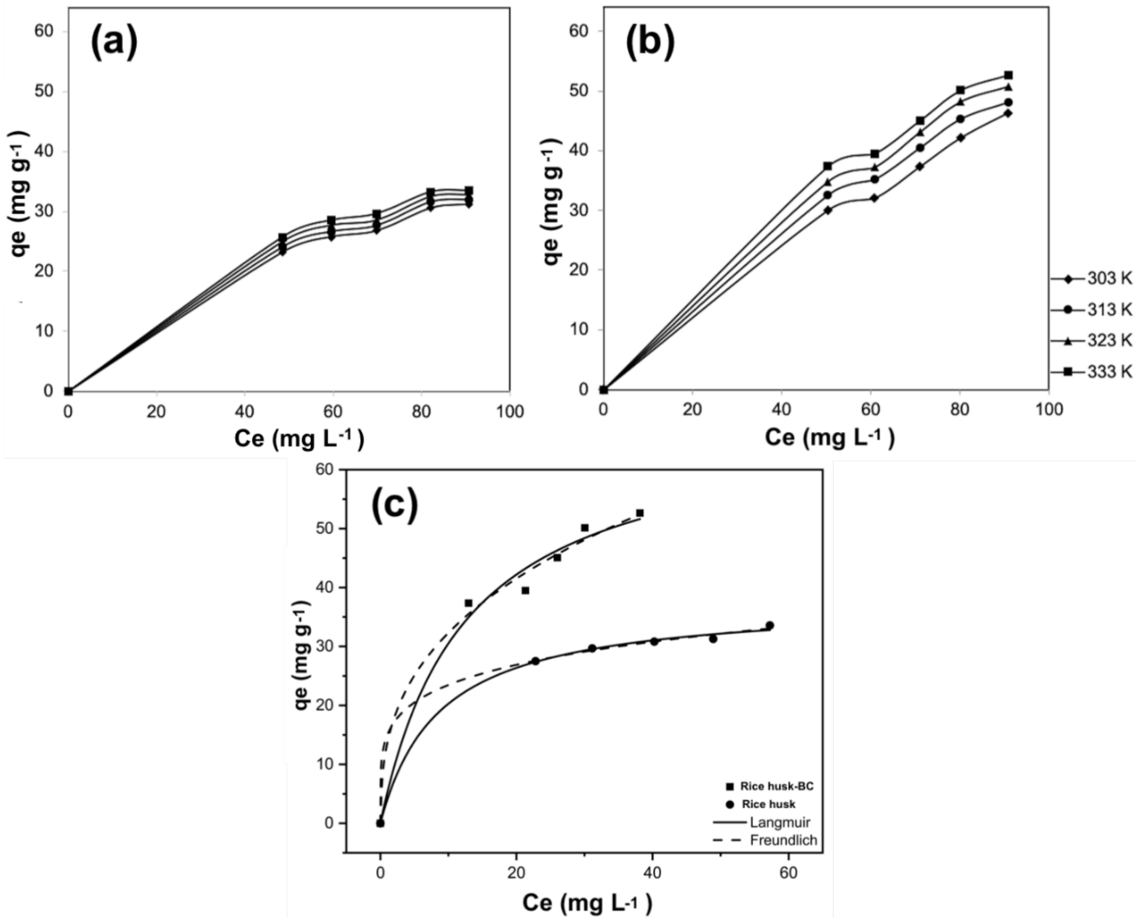

Figure 4 Effect of Procion Red concentration of rice husk (a) and rice husk-BC (b), and isotherm model (c).

Table 3 Results of equilibrium adsorption process, and thermodynamic parameters

Adsorbent	Isotherm Parameters		Thermodynamic parameters		
			ΔG (kJ mol^{-1})	ΔH (kJ mol^{-1})	ΔS (J mol^{-1} K^{-1})
Rice husk-BC	Q_{max}	84.034			
	$k_{Langmuir}$	0.027	-0.279		
	$R^2_{Langmuir}$	0.996	-0.670	11.560	0.039
	n	1.815	-1.671		
	$k_{Freundlich}$	5.705	-1.452		
	$R^2_{Freundlich}$	0.999			
Rice husk	Q_{max}	36.900			
	$k_{Langmuir}$	0.077	-0.120		
	$R^2_{Langmuir}$	0.986	-0.322	6.002	0.020
	n	3.789	-0.524		
	$k_{Freundlich}$	10.627	-0.726		
	$R^2_{Freundlich}$	0.999			

Table 4 Comparison of Procion Red adsorption using different adsorbents under various adsorption conditions

Ref	Adsorption capacity (mg g^{-1})	Adsorption condition	Adsorbents
[35]	5.26	50 mg/303 K/pH 3	Nat-Bentonite
[35]	9.97	50 mg/303 K/pH 3	Activated Bentonite
[17]	11.04	1 g/303 K	Montmorilonite
[15]	35.61	pH 2/303 K	*Bacilus Subtilis*
[46]	195	50 mg/pH 2/4 h	Pine Fruit Sheel
[18]	106	pH 2/50 mg	Homemade Peach
[47]	186	pH 2/298 K/78 mg/2h	Res. Deffated *Nigrospora Sp*
[11]	10.19	301 K/2 h/pH 5	Spirulina Algae
[19]	167	pH 6/303 K	Activeated-avocado shell
This research	84.034	333 K/50 mg/2 h	Rice husk-BC
This research	36.900	333 K/50 mg/2 h	Rice husk

The thermodynamic parameters are listed in Table 3; they are formulated in Eq. 5 and 6:

$$\Delta G = -RT \ln K_D \quad \text{(Eq. 5)}$$

$$\ln K_D = \frac{\Delta S}{R} - \frac{\Delta H}{RT} \quad \text{(Eq. 6)}$$

where K_D is the distribution coefficient, R is the molar gas constant, T is the absolute temperature (K), ΔH is the enthalpy (kJ mol^{-1}), ΔS is the entropy (J mol^{-1} K^{-1}), and ΔG is Gibbs value (kJ mol^{-1}). The spontaneity and feasibility of Procion Red removal by rice husk-BC and rice husk were confirmed by the negative Gibbs value. Increasing temperature leads to a decrease in the Gibbs value, which denotes the affinity of adsorbents to the dye molecule, with favourable conditions up to 333 K. According to Table 3, the adsorption of Procion Red using rice husk-BC and rice husk involves lower energy, indicating physisorption. The negative value of ΔG at various temperatures showed that the adsorption process is spontaneous, with the positive value of ΔH indicating that the adsorption process is endothermic. ΔH and ΔS for the liquid phase were affected by various conditions such as temperature, concentration, and interaction between liquid and solid interfaces during the adsorption process. In addition, the effect of temperature on adsorption was also found to depend on the viscosity of the solvent; with Procion Red, this will lead to higher mobility of the solute at higher temperatures. Thus, higher temperatures may be favourable for adsorption, with increased adsorption capacities. In addition, based on previous results [17], it is confirmed that the adsorption process follows the Langmuir isotherm, indicating adsorption of a monolayer on the surface, although the high adsorption capacity might suggest the formation of multiple layers. As previously reported by Ribeiro et al [49], for dye systems, the Langmuir assumptions of infinite dilution and monolayer saturation apply to gas systems with uniform sites and no interaction between monolayer adsorbed molecules on a homogeneous surface. This finding indicates that the interaction of the adsorbate and the adsorbent leads to effective adsorption of Procion Red.

3) Desorption and reusability

Desorption studies were performed, and reusability of the materials was then investigated by studying the effectiveness of the adsorbent after desorption. Figure 5 (A) shows the percentage of Procion Red desorption by several reagents. Among all the reagents used, ethanol produced the highest desorption, with a desorption percentage of up to 89%. Thus, the regeneration process is most effective when ethanol is used as the desorbing reagent. Experiments involving three cycles of adsorption-desorption were conducted. Figure 5 (B) shows the decrease in efficiency of adsorbents with each succeeding cycle; the first cycle showed a higher adsorption of Procion Red onto rice husk than onto rice husk-BC. The results indicated that Procion Red adsorption onto fresh rice husk-BC is 97% while it is only 34% after desorption. On the other hand, adsorption onto fresh rice husk was 69% and 50% after desorption. We assume that after the first desorption cycle, the adsorption capacity of rice husk-BC decreased; this may be because adsorbed Procion Red molecules are trapped in the active sites of rice husk-BC. However, it is observed that the rice husk-BC has better ability for regeneration after the first cycle as evident from the fact that adsorption percentage after the third cycle increases from 48% to 59%.

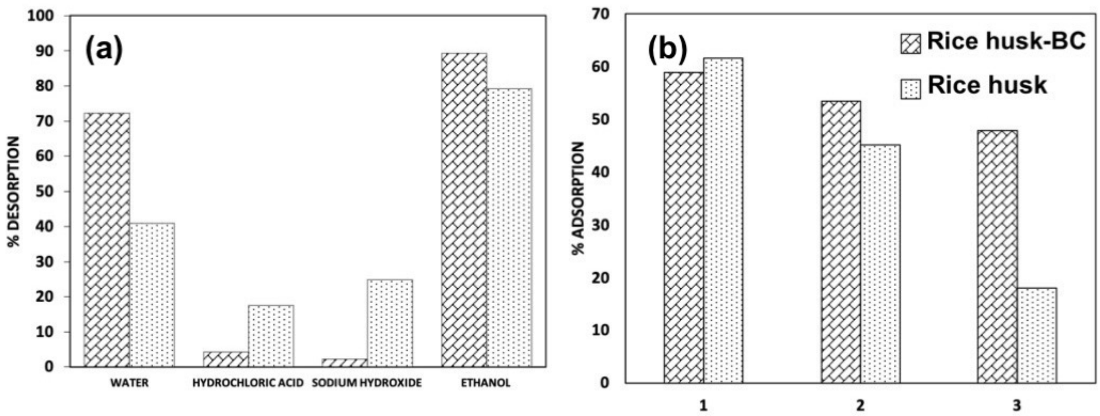

Figure 5 Graph of desorption (a) and reusability studies (b) of rice husk and rice husk-BC.

Conclusion

BC from rice husk was prepared and used as an effective biosorbent to remove Procion Red in the aqueous phase. The effectiveness of adsorption by rice husk-BC was examined using certain variables, including adsorption times, Procion Red concentration, and adsorption temperature settings. The adsorption processes of Procion Red onto both rice husk and rice husk-BC are demonstrated by the pseudo-second-order and Langmuir isotherm models. The increasing of adsorption maximum capacity in Q_{max} calculation from Langmuir model showed that rice husk has lower capacity than rice husk-BC which amount of Q_{max} is 36.900 mg g^{-1} to 84.034 mg g^{-1}. These findings can related that the rice husk-BC has large surface area specific. Furthermore, thermodynamic parameters indicated that the adsorption process was endothermic, spontaneous, and efficient at high temperatures. The regeneration of Procion Red adsorption showed the largest drop in the last cycle. Furthermore, these experimental are useful to increase the use of biomass as a potential adsorbent for wastewater treatment. The studied adsorbents are suitable to remove Procion red in an aqueous solution. besides that, the uses of agricultural waste as one source of potential can further help to reduce agricultural waste in the environment.

Acknowledgements

This study was supported "Hibah Profesi" Universitas Sriwijaya in fiscal year 2019–2021 by the financial support program for research with contract number 0014/UN9/SK.LP2M.PT/2019. Special thanks for Research Centre of Inorganic Materials and Complexes, Faculty of Mathematic and Natural Science Universitas Sriwijaya for analysis and instrumental supporting.

References

[1] Padhi, B.S., Ratna Pollution due to synthetic dyes toxicity & carcinogenicity studies and remediation. International Journal of Environmental Sciences, 2012, 3, 940–955.

[2] Lü, Z., Hu, F., Li, H., Zhang, X., Yu, S., Liu, M., Gao, C. Composite nanofiltration membrane with asymmetric selective separation layer for enhanced separation efficiency to anionic dye aqueous solution. Journal of Hazardous Materials, 2019, 19, 436–443.

[3] O'Connell, D.W., Birkinshaw, C., O'Dwyer, T.F. Heavy metal adsorbents prepared from the modification of cellulose: A review. Bioresource Technology, 2008, 99, 6709–6724.

[4] Yaseen, M., Singh, M., Ram, D. Growth, yield and economics of vetiver (Vetiveria zizanioides L. Nash) under intercropping system. Industrial Crops and Products, 2014, 61, 417–421.

[5] Vikrant, K., Giri, B.S., Raza, N., Roy, K., Kim, K.H., Rai, B.N., Singh, R.S. Recent advancements in bioremediation of dye: Current status and challenges. Bioresource Technology, 2018, 253, 355–367.

[6] Wang, C., Yediler, A., Lienert, D., Wang, Z., Kettrup, A. Toxicity evaluation of reactive dyestuffs, auxiliaries and selected effluents in textile finishing industry to luminescent bacteria Vibrio fischeri. Chemosphere, 2002, 46, 339–344.

[7] Zhang, P., Connor, D.O., Wang, Y., Jiang, L., Xia, T., Wang, L., …, Hou, D. A green biochar/iron oxide composite for methylene blue removal. Journal of Hazardous Materials, 2020, 384, 121286.

[8] Haile, H.L., Abi, T., Tesfahun, K. Synthesis, characterization and photocatalytic activity of $MnO_2/Al_2O_3/Fe_2O_3$ nano-composite for degradation of malachite green. African Journal of Pure and Applied Chemistry, 2015, 9, 211–222.

[9] Srinivasan, S., Sadasivam, S.K. Exploring docking and aerobic-microaerophilic biodegradation of textile azo dye by bacterial systems. Journal of Water Process Engineering, 2018, 22, 180–191.

[10] Gholami, P., Khataee, A., Soltani, R.D.C., Dinpazhoh, L., Bhatnagar, A. Photocatalytic degradation of gemifloxacin antibiotic using Zn-Co-LDH@biochar nanocomposite. Journal of Hazardous Materials, 2020, 382, 121070.

[11] Mohadi, R., Hanafiah, Z., Hermansyah, H., Zulkifli, H. Adsorption of procion red and congo red dyes using microalgae Spirulina sp. Science and Technology Indonesia, 2017, 2, 102–104.

[12] Boutemak, K., Taoualit, N., Cheknane, B., Laslouni, O. Djeddou, S., Medaoud, K., …, Aoudj, S. Equilibirum, kinetic and thermodynamic study of green malachite and rhodamine-B dyes sorption on olive pomace. Chemical Engineering Transactions, 2019, 73, 277–282.

[13] Lesbani, A., Taher, T., Palapa, N.R., Mohadi, R., Rachmat, A., Mardiyanto. Preparation and utilization of Keggin-type polyoxometalate intercalated Ni-Fe layered double hydroxides for enhanced adsorptive removal of cationic dye. SN Applied Sciences, 2020, 2, 470.

[14] Oktriyanti, M., Palapa, N.R., Lesbani, A. Effective removal of iron (II) from aqueous solution by adsorption using Zn/Cr layered double hydroxides intercalated with Keggin ion. Journal of Ecological Engineering, 2020, 21, 63–71.

[15] Binupriya, A.R., Sathishkumar, M., Ku, C.S., Yun, S.I. Biosorption of Procion Red MX 5B by Bacillus subtilis and its extracellular polysaccharide: Effect of immobilization. Clean - Soil, Air, Water, 2010, 38, 775–780.

[16] Nazifa, T.H., Habba, N., Salmiati, Aris, A., Hadibarata, A. Adsorption of Procion

Red MX-5B and crystal violet dyes from aqueous solution onto corncob activated carbon. Journal of the Chinese Chemical Society, 2018, 65, 259–270.

[17] Sarma, G.K., SenGupta, S., Bhattacharyya, K.G. Adsorption of Monoazo Dyes (Crocein Orange G and Procion Red MX5B) from water using raw and acid-treated montmorillonite K10: Insight into minetics, isotherm, and ithermodynamic parameters. Water, Air, and Soil Pollution, 2018, 229.

[18] Ribas, M.C., de Franco, M.A.E., Adebayo, M.A., Lima, E.C., Parkes, G.M.B., Feris, L.A. Adsorption of Procion Red MX-5B dye from aqueous solution using homemade peach and commercial activated carbons. Applied Water Science, 2020, 10, 1–13.

[19] Georgin, J., da Silva Marques, B., da Silveira Salla, J., Foletto, E.L., Allasia, D., Dotto, G.L. Removal of Procion Red dye from colored effluents using H_2SO_4-/HNO_3-treated avocado shells (Persea americana) as adsorbent. Environmental Science and Pollution Research, 2018, 25, 6429–6442.

[20] Xia, Y., Yang, T., Zhu, N., Li, D., Chen, Z., Lang, Q., …, Jiao, W. Enhanced adsorption of Pb(II) onto modified hydrochar: Modeling and mechanism analysis. Bioresource Technology, 2019, 288, 1–8.

[21] Lee, Y.C., Amini, M.H.M., Sulaiman, N.S., Mazlan, M., Boo, J.G. Batch adsorption and isothermic studies of malachite green dye adsorption using leucaena leucocephala biomass as potential adsorbent in water treatment. Songklanakarin Journal of Science and Technology, 2018, 40, 563–569.

[22] Abdulrazzaq, H., Jol, H., Husni, A., Abu-Bakr, R. Characterization and stabilisation of biochars obtained from empty fruit bunch, wood, and rice husk. BioResources, 2014, 9, 2888–2898.

[23] Gholami, P., Dinpazhoh, L., Khataee, A., Hassani, A., Bhatnagar, A. Facile hydrothermal synthesis of novel Fe-Cu layered double hydroxide/biochar nanocomposite with enhanced sonocatalytic activity for degradation of cefazolin sodium. Journal of Hazardous Materials, 2019, 120742.

[24] Kulaksiz, E., Gözmen, B., Kayan, B., Kalderis, D. Adsorption of Malachite Green on Fe-modified biochar: Influencing factors and process optimization. Desalination and Water Treatment, 2017, 74, 383–394.

[25] Aljeboree, A.M., Alshirifi, A.N., Alkaim, A.F. Kinetics and equilibrium study for the adsorption of textile dyes on coconut shell activated carbon. Arabian Journal of Chemistry, 2017, 10, S3381–S3393.

[26] Ríos-Badrán, I.M., Luzardo-Ocampo, I., García-Trejo, J.F., Santos-Cruz, J., Gutiérrez-Antonio, C. Production and characterization of fuel pellets from rice husk and wheat straw. Renewable Energy, 2020, 145, 500–507.

[27] Allen, S.J., Mckay, G., Porter, J.F. Adsorption isotherm models for basic dye adsorption by peat in single and binary component systems. Journal of Colloid and Interface Science, 2004, 280, 322–333.

[28] Hameed, B.H., El-Khaiary, M.I. Malachite green adsorption by rattan sawdust: Isotherm, kinetic and mechanism modeling. Journal of Hazardous Materials, 2008, 159, 574–579.

[29] Anshar, M., Kader, A.S., Ani, F.N. The utilization potential of rice husk as an alternative energy source for power plants in Indonesia. Advanced Materials Research, 2014, 845, 494–498.

[30] Yi, Q., Qi, F., Cheng, G., Zhang, Y., Xiao, B., Hu, Z., …, Xu, S. Thermogravimetric analysis of co-combustion of biomass and biochar. Journal of Thermal Analysis and Calorimetry, 2013, 112, 1475–1479.

[31] Siregar, P.M.S.B.N., Palapa, N.R., Wijaya, A., Fitri, E.S., Lesbani, A. Structural stability of Ni/Al layered double hydroxide supported on graphite and biochar toward adsorption of congo red. Science and Technology Indonesia, 2021, 6(2), 85–95.

[32] Chen, S., Qin, C., Wang, T., Chen, F., Li, X., Hou, H., Zhou, M. Study on the adsorption of dyestuffs with different properties by sludge-rice husk biochar: Adsorption capacity, isotherm, kinetic, thermodynamics and mechanism. Journal of Molecular Liquids, 2019, 285, 62–74.

[33] Ahmad, A., Khan, N., Giri, B.S., Chowdhary, P., Chaturvedi, P. Bioresource technology removal of methylene blue dye using rice husk, cow dung and sludge biochar: Characterization, application, and kinetic studies. Bioresource Technology, 2020, 123202.

[34] Luyen, N.T., Linh, H.X., Huy, T.Q. Preparation of rice husk biochar-based magnetic nanocomposite for effective removal of crystal violet. Journal of Electronic Materials, 2020, 49, 1142–1149.

[35] Taher, T., Rohendi, D., Mohadi, R., Lesbani, A. Thermal activated of Indonesian bentonite as a low-cost adsorbent for procion red removal from aqueous solution. The Journal of Pure and Applied Chemistry Research, 2018, 7, 79–93.

[36] Ntaflou, M., Vakros, J. Transesterification activity of modified biochars from spent malt rootlets using triacetin. Journal of Cleaner Production, 2020, 259, 120931.

[37] Kumar, R., Laskar, M.A., Hewaidy, I.F., Barakat, M.A. Modified adsorbents for removal of heavy metals from aqueous environment: A review. Earth Systems and Environment, 2019, 3, 83–93.

[38] Shi, H., Li, W., Zhong, L., Xu, C. Methylene blue adsorption from aqueous solution by magnetic cellulose/graphene oxide composite: Equilibrium, kinetics, and thermodynamics. Industrial and Engineering Chemistry Research, 2014, 53, 1108–1118.

[39] Hu, Z., Cai, L., Liang, J., Guo, X., Li, W., Huang, Z. Green synthesis of expanded graphite/layered double hydroxides nanocomposites and their application in adsorption removal of Cr(VI) from aqueous solution. Journal of Cleaner Production, 2019, 209, 1216–1227.

[40] Yalc, N., Sevinc, V. Studies on silica obtained from rice husk. 2001, 27, 219–224.

[41] Liu, Y., Zhao, X., Li, J., Ma, D., Han, R. Characterization of bio-char from pyrolysis of wheat straw and its evaluation on methylene blue adsorption. Desalination and Water Treatment, 2014, 46, 115–123.

[42] Li, Y., Bi, H.Y., Liang, Y.Q., Mao, X.M., Li, H. A magnetic core-shell dodecyl sulfate intercalated layered double hydroxide nanocomposite for the adsorption of cationic and anionic organic dyes. Applied Clay Science, 2019, 183, 105309.

[43] Shenvi, S.S., Isloor, A.M., Ismail, A.F., Shilton, S.J., Ahmed, A.A. Humic acid based biopolymeric membrane for effective removal of methylene blue and Rhodamine B. Industrial and Engineering Chemistry Research, 2015, 54, 4965–4975.

[44] Liu, Z., Zhang, F.S. Removal of lead from water using biochars prepared from hydrothermal liquefaction of biomass. Journal of Hazardous Materials, 2009, 167, 933–939.

[45] Nekouei, F., Kargarzadeh, H., Nekouei, S., Tyagi, I., Agarwal, S., Gupta, V.K. Preparation of nickel hydroxide nanoplates modified activated carbon for malachite green removal from solutions: Kinetic, thermodynamic, isotherm and antibacterial studies. Process Safety and Environmental Protection, 2016, 102, 85–97.

[46] Calvete, T., Lima, E.C., Cardoso, N.F., Dias, S.L.P., Pavan, F.A. Application of carbon adsorbents prepared from the

Brazilian pine-fruit-shell for the removal of Procion Red MX 3B from aqueous solution-Kinetic, equilibrium, and thermodynamic studies. Chemical Engineering Journal, 2009, 155, 627–636.

[47] Tonato, D., Drumm, F.C., Grassi, P., Georgin, J., Gerhardt, A.E., Dotto, G.L., Mazutti, M.A. Residual biomass of Nigrospora sp. from process of the microbial oil extraction for the biosorption of procion red H–E7B dye. Journal of Water Process Engineering, 2019, 31, 100818.

[48] Palapa, N.R., Juleanti, N., Normah, Mohadi, R., Taher, T., Rachmat, A., Lesbani, A. Copper aluminum layered double hydroxide modified by biochar and its application as an adsorbent for Procion Red. Journal of Water and Environment Technology, 2020, 18, 359–371.

[49] Ribeiro, C., Scheufele, F.B., Espinoza-Quiñones, F.R., Módenes, A.N., da Silva, M.G.C., Vieira, M.G.A., Borba, C.E. Characterization of Oreochromis niloticus fish scales and assessment of their potential on the adsorption of reactive blue 5G dye. Colloids and Surfaces A: Physicochemical and Engineering Aspects, 2015, 482, 693–701.